ELSEVIER

International Journal of Solids and Structures 41 (2004) 4635–4659

INTERNATIONAL JOURNAL OF SOLIDS and STRUCTURES

www.elsevier.com/locate/ijsolstr

Analytical solution to the plate impact problem of layered heterogeneous material systems

X. Chen [a], N. Chandra [a,*], A.M. Rajendran [b]

[a] *Department of Mechanical Engineering, Florida State University, 2525 Pottsdamer St., Tallahassee, FL 32310, USA*
[b] *Army Research Office, Engineering Science Directorate Research Triangle Park, NC 27709, USA*

Received 25 July 2003; received in revised form 26 February 2004
Available online 27 April 2004

Abstract

An analytical solution to the problem of one-dimensional high amplitude wave propagation in layered heterogeneous material systems has been developed, based on Floquet's theory of ODEs with periodic coefficients. The problem is formulated based on a conventional plate impact experimental configuration. In a plate impact test, the boundary condition at the plane of the impact varies with time as a result of multiple wave interactions at the interfaces of the layered target material. The approach of the solution is to convert the initial velocity boundary value problem to a time-dependent stress boundary value problem and then obtain the stress time history by means of superposition. By taking this approach, we explicitly consider multiple wave interactions at the heterogeneous interfaces. A characteristic steady-state stress σ_{mean} for heterogenous material has been identified which is quite different from σ_0 the stress at the initial time of impact. It is shown that σ_{mean} can be obtained by summing up the stress increments at the interfaces or by using mixture theory. The late-time (steady-state) solution procedures for the plate impact problem are presented for impact velocities corresponding to elastic as well as shock wave loading conditions. Results from the analytical model compare well with both numerical results obtained from a shock wave based finite element code and experimental data.
© 2004 Elsevier Ltd. All rights reserved.

Keywords: Wave interactions; Layered heterogeneous material systems; Shock response; Plate impact

1. Introduction

In order to characterize the dynamic behavior of materials under impact loading, diagnostic experiments are usually carried out using a plate impact test configuration under a one-dimensional strain state. The plate impact test serves the exact purpose of characterizing materials under high-pressure dynamic loading, analogous to that of uniaxial tensile tests under quasi-static loading conditions. In a plate impact test, the stress response is usually measured at intermediate locations within a given specimen using embedded

* Corresponding author. Tel.: +1-8504106320; fax: +1-8504106337.
E-mail address: chandra@eng.fsu.edu (N. Chandra).

0020-7683/$ - see front matter © 2004 Elsevier Ltd. All rights reserved.
doi:10.1016/j.ijsolstr.2004.02.064

manganin or PVDF gauges, while the velocity measurements are typically carried out using a velocity interferometry (VISAR) system at the stress free back surface of the target plate, or at the interface of a transparent window glued to the back of the target plate. These well-structured wave profiles in metals and ceramics provide a wealth of information about the shock response of the material. Since engineered composites such as glass reinforced plastic (GRP) comprise complex microstructures, wave scattering occurs due to multiple wave interactions at interfaces. The description of scattering process in a real composite is very complicated and extremely difficult to analyze. It has been recognized that a periodically layered system offers a practical configuration to investigate the effect of heterogeneity of general composites. Wave propagation in a periodically layered medium has been studied extensively for decades. Historically, theoretical work on wave propagation studies in layered systems has followed the mathematical solution to ordinary differential equations with periodic coefficients attributed to Floquet that dates back to 1800s. As early as 1956, Rytov obtained a dispersion relation for one-dimensional longitudinal waves propagating in a periodic laminate. Later, by using the effective stiffness theory Sun et al. (1968) obtained the dispersion relations for harmonic waves propagating parallel and normal to the direction of the layering. Peck and Gurtman (1969) studied the wave propagation parallel to the layers, and obtained the asymptotic solution through approximation under similar loading conditions. Sve (1972) and Chen and Clifton (1975) predicted the late-time asymptotic solutions and the wave front solution for wave propagation normal to the layers for unit step loading at the boundary. Ting (1980) developed an analytical solution for unit step loading for viscoelastic layered media at finite locations.

The above-mentioned analytical works of wave propagation in layered material systems have either used a sinusoidal wave loading, or unit step loading. There are no known analytical solutions for plate impact loading conditions. The main objective of this paper is to present a solution methodology based on Floquet's theory for plate impact loading problems. The background section presents a brief description of the plate impact test configuration as well as a summary of earlier work relating to wave propagation analysis for layered material systems. In Section 3 we develop the basic formulation for plate impact problem and propose solution procedures. In Section 3.3 we compare the analytical results with experimental data. In the final section we summarize the paper.

2. Background

A schematic of the compressive stress history (measured using an embedded stress gauge) is shown in Fig. 1. The portion of the plot indicated by the letter A represents the arrival of an elastic shock wave from the impact plane. The material particles are compressed elastically (A–C) until the relatively slow moving plastic shock wave arrives at the given location. Typically, the shape and time duration of the portion A–C depends on the strain rate sensitivity of the material and the distance from the impact plane. If the shock

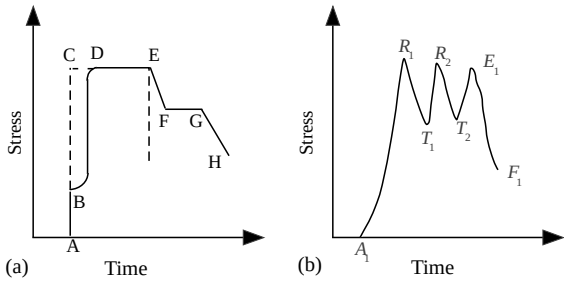

Fig. 1. Schematic wave profiles of homogeneous metals and layered composites for a finite thickness flyer plate: (a) homogeneous metals and (b) layered composites.

amplitude is below the elastic limit, the profile typically follows portions AC–CE. The rise time is usually of the order of nanoseconds for metals and ceramics. If the shock amplitude is above the elastic limit, then the plastic shock takes the stress to the peak between points D and E. The peak level remains the same until the elastic unloading wave arrives from the back of the flyer plate. Often, the release portion of the wave profile exhibits a typical structure that consists of elastic release (E–F), transition (F–G), and plastic release (G–H). Fig. 1(b) shows schematic of a typical shock response of a layered composite system. Interpretation of this profile is extremely difficult without a careful wave analysis. Since stress or velocity profiles is a result of superpositions of numerous wave reflections at the interfaces, the stress level at R_1 is an intermediate stress state. A_1R_1 shows a dispersed wave structure with longer rise time compared to the rise time in a target plate of a homogeneous material. The oscillatory portion R_1–E_1 at the peak level indicates arrivals of several release and compressive waves. The pulse duration becomes a function of not only the thickness and wave speed in the flyer plate, but also on the number of interfaces and wave speeds in the heterogeneous system. In layered systems, planar interfaces interact with the incident shock wave generating transmitted and reflected waves, their amplitudes being determined by the impedance mismatch. This factor should be explicitly considered in evaluating the shock response of layered systems.

Table 1 summarizes major past work that studied wave profiles in alternating layered systems using the plate impact test configuration. Lundergan and Drumheller (1971) numerically simulated the response of a layered material system with varying thickness. The simulated particle velocity response exhibited a slow rise time and an oscillatory behavior as observed in experiments. The idea of replacing the dispersive, heterogeneous composite with an equivalent homogeneous dissipative continuum was first proposed by Barker (1971). A general nonlinear Maxwell (viscous) model was proposed to simulate stress relaxation from an instantaneous state of the mixture to the equilibrium level. In addition, Barker obtained oscillatory stress solutions by explicitly modeling each layer using a stress wave propagation based one-dimensional code. Barker validated the viscous model for the composite equation of state by successfully matching the averaged stress response in the oscillations from the code. Barker et al. (1974) further validated his theory using results from experiments in which a low volume fraction of aluminum was used in a PMMA/aluminum based layered system. However, in general this model fails to predict the structure of the stress waves (rise time, peak stress and oscillations).

While carrying out impact experiments on layered Cu/PMMA systems, Oved et al. (1978) (see Table 1) noticed significant oscillations in the stress wave profiles. As can be seen in the corresponding figure, the oscillations occur approximately about a mean stress. When the amplitude of oscillations is substantial, Oved pointed out that oscillations do not vanish with distance of propagation in the shock regime. Consequently, oscillations should not be ignored but it should be explicitly modeled. More recently Kanel et al. (1995) confirmed the harmonic oscillations in experiments on a Cu/PE system. They proposed a relaxation model similar to that of Barker, though the physics behind the models is quite different. The main thrust of Kanel's approach was to obtain the nonequilibrium pressure (the difference between the Rayleigh line to the final state and the equilibrium pressure corresponding to the Hugoniot curve) by assuming an empirical kinetic relationship.

Dandekar and Beaulieu (1995) reported results from plate impact tests on a woven fabric composite. The measured VISAR signal revealed an oscillatory peak stress behavior and a long rise time. Boteler et al. (1999) further conducted a combined experimental and computational study on stress attenuation and dispersion in GRP laminates. The stress profiles at three different distances from the impact plane were measured using embedded PVDF gauges. They observed that the rise time increased and the average peak stress reduced with propagation distance. Some oscillations were observed at the peak stress in the first gauge, which was closer to the impact plane. Stress histories at locations significantly away from the impact plane showed no oscillatory behavior at the peak level. Their computational modeling using a three dimensional viscoelastic model matched the attenuation of the stress, but failed to reproduce wave dispersions.

Table 1
Review of major past work done in studying wave profiles in alternating layered systems under plate impact

Author/year	Material system (target) Experiment/ simulation configuration	Observations or results	Method/model
Lundergan and Drumheller (1971)	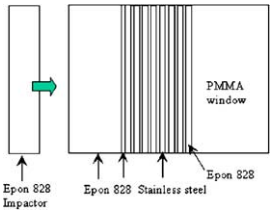	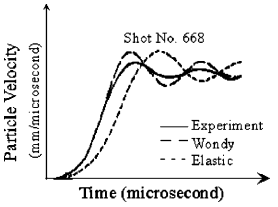	
Barker et al. (1974)	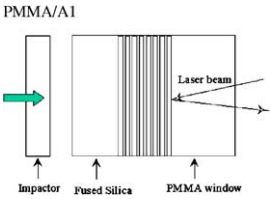	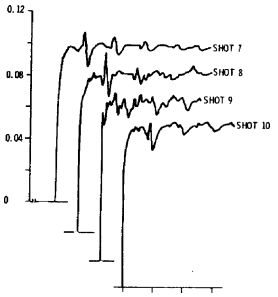	Viscous model (Maxwell model)
Oved et al. (1978)	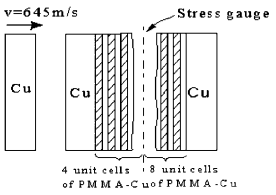	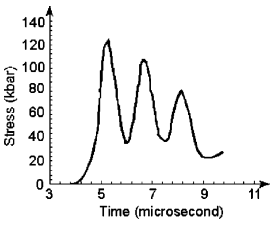	Numerical analysis + experiments
Kanel et al. (1995)	Cu/PE, Al/PE, W/Al Not available	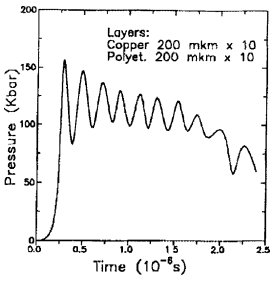	Viscous model based on the Hugoniot curve.
Clements et al. (1996)	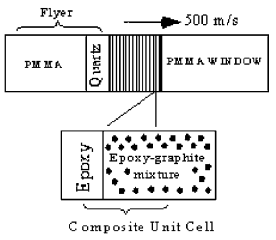	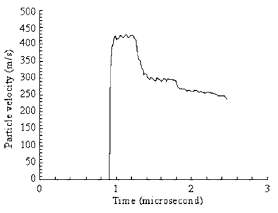	Unit cell method

Table 1 (*continued*)

Author/year	Material system (target) Experiment/ simulation configuration	Observations or results	Method/model
Boteler et al. (1999)	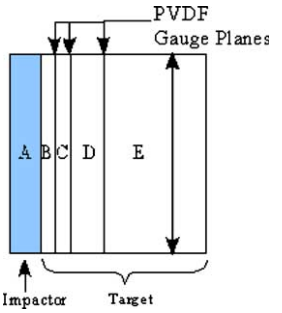	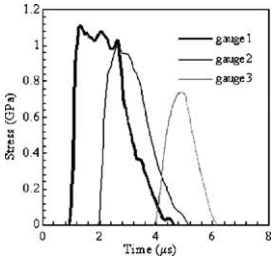	3D Linear viscoelastic model
Dandekar and Beaulieu (1995) and Espinosa et al. (2000)	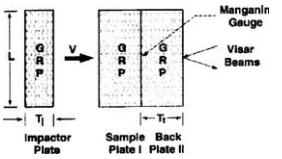	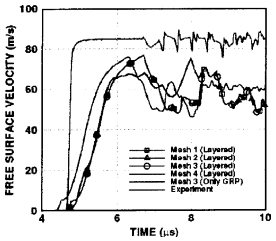	Cohesive zone model + layered configuration
Zhuang (2002)	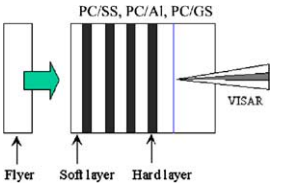	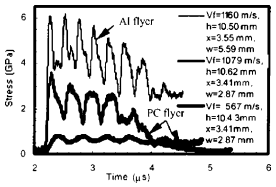	Applying Dremin's mixture theory for analysis

Clements et al. (1996) proposed a modified unit cell method to model wave propagation in alternating Epoxy and Epoxy-graphite system. Recently, Zhuang (Zhuang, 2002; Zhuang et al., 2003) conducted a thorough experimental investigation by performing a large number of plate impact experiments in selected material systems involving alternate units of either polycarbonate and stainless steel or polycarbonate and glass. Both the quasi-harmonic oscillations and the finite rise time were observed in different systems. The effects of impedance mismatch, interface density, propagation distance as well as loading strength were examined as the basic parameters in his experiments.

In the study of wave propagation in solids, scattering, dispersion and attenuation play critical roles in determining the thermomechanical response of the media. These phenomena can be attributed to a number of nonlinearities arising from the wave characteristics, loading conditions and material heterogeneity (at various spatial scales ranging from nanometers to a few millimeters). The nonlinear effects in general can be ascribed to impedance (and geometric) mismatch at various length scales as often encountered in composite material systems. In addition, material nonlinearities (inelastic effects) can arise due to void nucleation and growth, microcracking, and delamination. The strong shock waves generated under high velocity impact loading often induce nonlinear effects in the deformation and failure behaviors (Nesterenko, 2001).

Present authors (Chandra et al., 2002) showed that the observed structures in the measured stress wave profiles in layered systems under low velocity impact loading condition could be explained through

modeling the scattering effects at planar interfaces. However, for high velocity impact loading conditions, it is fully realized that material nonlinear effects may play a key role in altering the basic structure. Therefore, it is important that models that describe the wave structures include equation of state for each material in the periodic layered system, in the shock wave regime.

3. Problem formulation and solution method

3.1. Formulation

Consider two semi-infinite bodies Ω_1 $(-\infty < y,z < \infty, 06x < \infty)$ and Ω_2 $(-\infty < y,z < \infty, -\infty < x < 0)$ such that they are initially separated and then impact each other with velocity $\vec{v} = v_0\vec{i}$ in the x-direction, as shown in Fig. 2(a). Without loss of generality, we can assume Ω_1 to be fixed in space and Ω_2 impacting on the entire $x = 0$ plane. Upon impact, stress waves are generated on a plane parallel to the impact plane and travel in the negative x-direction in Ω_2 positive x-direction in Ω_1 with wave velocities determined by the material properties of these two bodies. The amplitude or strength of the stress wave is determined by the velocity of impact v_0 and acoustic impedances of Ω_1 and Ω_2. As the waves propagate away from the impact plane, bodies Ω_1 and Ω_2 are in compression with a uniaxial state of strain $\varepsilon_x \neq 0$ and all other components $\varepsilon_{ij} = 0$ (for $i,j = 1,2,3$ except $i = j = 1$). The problem is to find the state of strain and stress in the compressed regions, given the velocity of impact and the material properties of the two bodies.

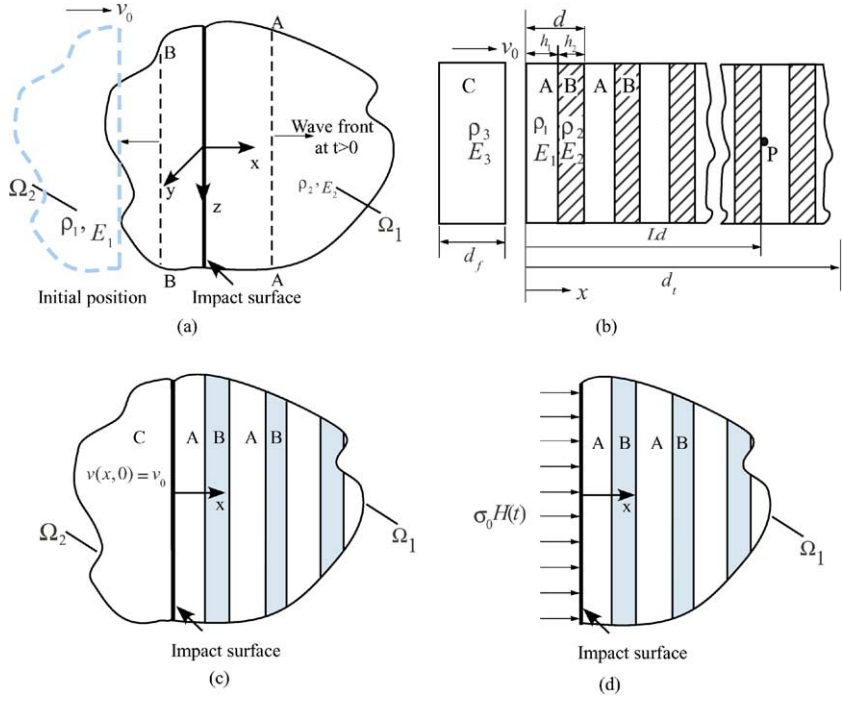

Fig. 2. Schematic of the configuration for impact problem: (a) two half spaces of homogeneous materials; (b) general plate impact problem of layered systems; (c) plate impact problem of two half spaces with target being layered and (d) the layered media under unit step loading.

This plate impact problem has long been well understood and successfully modeled when Ω_1 and Ω_2 are homogeneous. What we seek here is a solution to the problem when Ω_1 is laminated as shown in Fig. 2(c) as a precursor to the practical plate impact test shown in Fig. 2(b). In the plate impact test (Fig. 2(b)), Ω_2 is called flyer plate or the impactor impacting on Ω_1, termed target plate. The target plate is made of alternating layers of materials A and B with the impactor made of a homogeneous material C. All the materials (layers) are assumed to be homogeneous and damage free with known mechanical (E, v) and physical (ρ, and equation of state) properties. Though the bulk of the paper assumes a constitutive relationship of linear elastic, isotropic form, extensions to very high stress regimes are formulated by invoking the equation of state.

In this work, we seek the stress history in Ω_1, as posed in Fig. 2(b). This problem is identical to the problem in Fig. 2(c) if the thickness of the flyer plate (d_f) and the target plate (d_t), and the lateral dimensions (radius of the plates) are large enough not to permit wave reflections from the free surfaces to interfere with the solution. In other words, the strain state remains strictly one dimensional for the solution time duration.

The governing equations can be written as follows:

Equation of motion

$$\frac{\partial \sigma(x,t)}{\partial x} = \rho_i \frac{\partial^2 u(x,t)}{\partial t^2}. \tag{1}$$

Velocity continuity

$$\frac{\partial \varepsilon(x,t)}{\partial t} - \frac{\partial v(x,t)}{\partial x} = 0. \tag{2}$$

Constitutive relation (elastic laminates)

$$\sigma(x,t) = E_i \varepsilon(x,t), \tag{3}$$

where $\sigma(x,t)$, $u(x,t)$, $v(x,t)$ and $\varepsilon(x,t)$ denote the longitudinal stress, displacement, velocity and strain, respectively. As shown in Fig. 2(b), the constants ρ_i and E_i $(i = 1, 2, 3)$ represent the material densities and the elastic moduli for the uniaxial strain of materials A, B and C, respectively.

Initial boundary condition

Stress, displacement and strain are zero in Ω_1 and Ω_2 at $t = 0^-$

$$\begin{cases} \sigma(x,0) = 0 \\ u(x,0) = 0 \quad \text{for } -\infty < x < \infty. \\ \varepsilon(x,0) = 0 \end{cases} \tag{4}$$

Initial velocity condition

$$v(x,0) = v_0 \quad \text{for } x < 0. \tag{5}$$

Stress and velocity continuity (at all interfaces)

For wave propagation in a layered medium, the stress and displacement continuity should be maintained at all interfaces

(a) stress continuity at $x = h_1 + Ld$

$$\sigma_a(h_1 + Ld, t) = \sigma_b(h_1 + Ld, t), \tag{6}$$

where L is a positive integer representing the number of unit cells and h_i $(i = 1, 2)$, are the thickness of layer 1 and layer 2, and the d is the thickness of the unit cell with $d = h_1 + h_2$;

(b) stress continuity at $x = Ld$

$$\sigma_a(Ld,t) = \sigma_b(Ld,t). \tag{7}$$

In the same manner, velocity continuity at $x = h_1 + Ld$ and $x = Ld$

$$v_a(h_1 + Ld,t) = v_b(h_1 + Ld,t), \tag{8}$$

$$v_a(Ld,t) = v_b(Ld,t). \tag{9}$$

3.2. Solution method

Before we formulate a solution method to the problem prescribed in Eqs. (1)–(9) it is instructive to garner the prevailing solutions to closely related problems. The earliest useful work is the Floquet's theory (1880) to a system of ordinary differential equations (ODEs) with periodic coefficients. Solutions to those ODEs can be written as a set of functions with the same period as the problem. Rytov (1956), Sve (1972), Chen and Clifton (1975) used Floquet's theory, when stress in the form of a Heaviside function is applied to Ω_1, as shown in Fig. 2(d). These works are very important for the present development; however, the boundary condition of unit step loading is quite different from that prescribed in Fig. 2(b) and it substantially alters the final results. In a recent paper (Chandra et al., 2002), the present authors have formulated the problem as a sequence of scattering events at each of the interfaces A–B–A... and developed a solution to the strength of the propagating waves as a function of time and space.

3.2.1. The late-time solution for unit step loading

We seek velocity or/and stress as a function of time at any given location. Thus the solution is of the form $v = v(x,t)$ and $\sigma = \sigma(x,t)$. The time domain in the governing equations (1)–(9) is now converted to frequency domain through the Laplace transform. Then by invoking Floquet's theory and also considering the stress and velocity continuity at $x = h_1$ and $x = d$ based on Eqs. (6)–(9), we can obtain the dispersion relation (for details see Appendix A)

$$\cosh kd = \cosh\frac{s}{c_1}h_1 \cosh\frac{s}{c_2}h_2 + \frac{1}{2}\left(\frac{\rho_1 c_1}{\rho_2 c_2} + \frac{\rho_2 c_2}{\rho_1 c_1}\right)\sinh\frac{s}{c_1}h_1 \sinh\frac{s}{c_2}h_2, \tag{10}$$

where k is effective wave number for waves in the laminates, s is the frequency of the wave in layer A and layer B, where h_1,h_2 and c_1, c_2 are thicknesses and longitudinal wave velocities of layers A and B, respectively. Eq. (10) describes the effective sound wave number k of laminates in terms of velocities c_1 and c_2 in each layer for a given frequency s, and is thus termed as 'dispersion relation'.

From Eq. (10) we can obtain the phase velocity at zero frequency limit by letting frequency $s \to 0$ (or time $t \to \delta$). Thus

$$c_0 = \frac{d}{\left[\left(\frac{h_1}{c_1}\right)^2 + \left(\frac{h_2}{c_2}\right)^2 + \left(\frac{\rho_1 c_1}{\rho_2 c_2} + \frac{\rho_2 c_2}{\rho_1 c_1}\right)\frac{h_1 h_2}{c_1 c_2}\right]^{1/2}}, \tag{11}$$

where c_0 is the phase velocity at the zero frequency limit for the laminated system (as shown in Eq. (11)). It should be noted that above equation is obtained by letting $t \to \infty$, and consequently valid for large propagation distance. The above solution is independent of the boundary condition, and thus Eq. (11) is equally valid for both plate impact and unit step loading.

For unit step loading (see Fig. 2(d)), the stress boundary condition for the target plate is

$$\sigma(0,t) = \sigma_0 H(t), \tag{12}$$

where σ_0 is the applied stress on the boundary of the laminates. The solution of the stress response at $x = Ld$ can be obtained by evaluating the integral from the inverse of Laplace transform

$$\sigma(Ld,t) = \frac{1}{2\pi \mathrm{i}} \int_{\gamma-\mathrm{i}\infty}^{\gamma+\mathrm{i}\infty} \bar{\sigma}(Ld,s)\mathrm{e}^{st}\,\mathrm{d}s. \tag{13}$$

Now let a small time-scale δ be defined as

$$\delta = t - x/c_0. \tag{14}$$

By introducing δ, we remove the variable x from the stress function shown in Eq. (13). Substituting Eqs. (14) into (13) and assuming $p(t,\delta)$ is the stress function with t, δ as the variables

$$p(t,\delta) = \frac{\sigma_0}{2\pi \mathrm{i}} \int_{\gamma-\mathrm{i}\infty}^{\gamma+\mathrm{i}\infty} \frac{\mathrm{e}^{-\delta g(s)}\mathrm{e}^{th(s)}\,\mathrm{d}s}{s}, \tag{15}$$

where

$$g(s) = k(s)c_0,$$

$$h(s) = g(s) + s = k(s)c_0 + s.$$

We seek an asymptotic representation of $p(t,\delta)$ for $t \to \infty$. Such representation can be obtained by making the integration path following a path of steepest descent through the saddle point s_0 at which $h'(s) = 0$. This happens when $s \to 0$. Evaluation of the integral in Eq. (15) finally gives an integral of the Airy function, so the overall stress history at x is given by

$$\sigma(x,t) = \sigma_0 \left[\frac{1}{3} + \int_0^B A\mathrm{i}(-s)\,\mathrm{d}s \right], \tag{16}$$

where

$$B = \left(t - \frac{x}{c_0} \right) \left(\frac{2}{h'''(0)t} \right)^{1/3} \tag{17}$$

and

$$h'''(0) = \frac{(c_0)^2}{d^2} \left\{ \left(\frac{h_1}{c_1} \right)^2 \left(\frac{h_2}{c_2} \right)^2 \left[1/4 \left(\frac{\rho_1 c_1}{\rho_2 c_2} + \frac{\rho_2 c_2}{\rho_1 c_1} \right)^2 - 1 \right] \right\}. \tag{18}$$

It should be noted that Sve (1972) evaluated an integral analogous to Eq. (15) and obtained the same solution as above. But the above solution for unit step loading is given by Chen and Clifton's (1975) work, and the details are shown in Appendix A.

Eq. (16) provides the solution to the stress profile of a laminated system subjected to a unit step loading. Though it is tempting to specify the amplitude of this step as the stress at the impact plane at the time of impact, it will be shown later that this is not correct. Despite this, the stress response of a unit step loading on bilaminates qualitatively displays all the essential features found in plate impact tests. Consider the case of bilaminates with material A as PMMA with $h_1 = 0.26$ mm and B as copper with $h_2 = 0.36$ mm. When subjected to unit step loading given by Eq. (12), the stress history at $x = 10$ mm can be calculated using Eqs. (16) and (18). Fig. 3 shows the stress history. It should be noted that the effective speed of c_0 is the wave velocity that corresponds to a stress level of $\frac{1}{3}\sigma_0$. It can be seen that the stress rises with a specific slope (as opposed to a vertical rise for a homogenized material). Then the stress oscillates about an average stress equivalent to the applied stress σ_0. In addition, the oscillations are almost harmonic with the amplitude of oscillations decaying with time.

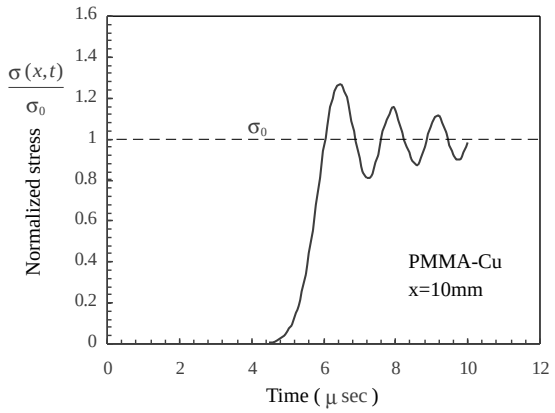

Fig. 3. Solution to the unit step loading condition in PMMA-Cu.

3.2.2. Solution to the plate impact problem

Problem as shown in Fig. 2(c) describes the plate impact problem while late-time solution in the previous section pertains to problem in Fig. 2(d). For a plate impact test, the body Ω_2 is continuously in contact with Ω_1 imposing initially a velocity boundary condition at $x = 0$ and at $t = 0$, compared to the constant stress boundary condition in Fig. 2(d). However, for problems in Fig. 2(c) the magnitude of loading on the boundary of the target plate keeps changing due to wave reflections in the target plate. Let us suppose σ_0 be the stress induced at the time of impact between C and A. As shown below, additional stress increments are induced at the impact plane due to wave reflections from interfaces.

In this section, we formulate the stress increments as a function of impedance mismatch between the materials A and B, and between materials C and A.

Incident wave. Upon initial impact of Ω_2 on Ω_1, the incident wave with magnitude σ_0 is generated at the impact instant, and the magnitude σ_0 is given by

$$\sigma_0 = \frac{\rho_3 c_3 \rho_1 c_1 v_0}{\rho_3 c_3 + \rho_1 c_1}. \tag{19}$$

Second wave train. Fig. 4(a) shows the schematics of the wave traveling within the target body Ω_1. The incident wave first travels in material A. As it reaches the interface A–B, part of it is reflected back and the rest of it is transmitted (shown in dotted line only for wave train 'a'). This reflected wave arrives back at the impact plane after a time $t_{\sigma_1} = 2t_a = 2h_1/c_1$. Stress at the impact plane is altered by this new wave arrival given by

$$\Delta\sigma_1 = r_{A\text{–}B}(1 + r_{A\text{–}C})\sigma_0, \tag{20}$$

where $r_{A\text{–}B} = \frac{\rho_2 c_2 - \rho_1 c_1}{\rho_1 c_1 + \rho_2 c_2}$ and $r_{A\text{–}C} = \frac{\rho_3 c_3 - \rho_1 c_1}{\rho_1 c_1 + \rho_3 c_3}$ are the reflection ratios at interface A–B and C–A, respectively. Here C is the flyer plate. The cumulative stress level up to the second wave train at $x = 0$ at $t_{\sigma_1} = 2t_a = 2h_1/c_1$ is

$$\sigma_1 = \sigma_0 + \Delta\sigma_1 = [r_{A\text{–}B}(1 + r_{A\text{–}C}) + 1]\sigma_0. \tag{21}$$

Third wave train. The propagation path of the third wave train depends on the ratio of the transit time in layer $A(t_a)$ and that in layer $B(t_b)$.

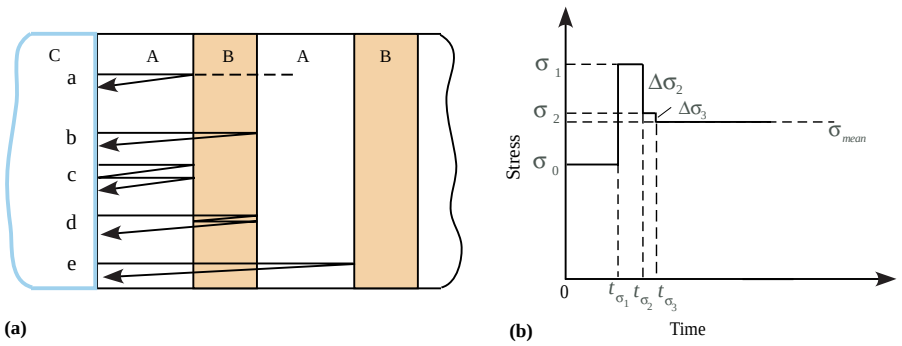

Fig. 4. Multi-step loading method: (a) the wave trains that reach the impact plane from inside of the target due to reflections and (b) the equivalent loading history of the target plate.

(a) If $t_a = (\frac{h_1}{c_1}) > t_b = (\frac{h_2}{c_2})$, then the third wave train comes from the branch that has one reflection in layer B and reaches the boundary at $t = 2t_a + 2t_b$, which is represented as path b in Fig. 4 (a). The stress variation due to the wave train that follows this path can be calculated as

$$\Delta\sigma_2 = [r_{A\text{–}B}(1 - r_{A\text{–}B}^2)(1 + r_{A\text{–}C})]\sigma_0. \tag{22}$$

So, the overall stress magnitude up to the third wave train (still at the impact plane) is

$$\sigma_2 = \sigma_1 + \Delta\sigma_2. \tag{23}$$

(b) If $t_a = \left(\frac{h_1}{c_1}\right) < t_b = \left(\frac{h_2}{c_2}\right)$, then the third wave train follows path c, which goes through two reflections in layer A and reaches the impact plane at time $t_{\sigma_2} = 4h_1/c_1$

$$\Delta\sigma_2' = r_{A\text{–}B}^2 r_{A\text{–}C}(1 + r_{A\text{–}C})\sigma_0. \tag{24}$$

The overall stress is

$$\sigma_2 = \sigma_1 + \Delta\sigma_2'. \tag{25}$$

(c) When $t_a = \left(\frac{h_1}{c_1}\right) = t_b = \left(\frac{h_2}{c_2}\right)$, the propagating path of the wave trains is independent of the materials. So the third wave train comprises waves that follow path b and waves that follow path c. As a result, the increment of this wave trains $\Delta\sigma_2''$ are the sum of Eq. (22) and Eq. (24), so we have

$$\sigma_2 = \sigma_1 + \Delta\sigma_2'' = \sigma_1 + \Delta\sigma_2 + \Delta\sigma_2'. \tag{26}$$

Fourth wave train. The propagation path of the fourth wave train that reaches the boundary of the target plate still depends on the transit times t_a and t_b. For example, if $t_a > 2t_b$, then the fourth wave train follows path d and arrives at the boundary at time $t_{\sigma_3} = 2t_a + 4t_b$, as shown in Fig. 4, can be obtained by

$$\Delta\sigma_3 = [r_{A\text{–}B}^3(1 - r_{A\text{–}B}^2)(1 + r_{A\text{–}C})]\sigma_0. \tag{27}$$

And the overall stress up to the third wave train σ_3 is

$$\sigma_3 = \sigma_2 + \Delta\sigma_3. \tag{28}$$

Also, if $t_a = t_b$, then the fourth wave train contains the waves that follow either path d or path e.

The fifth, sixth and additional wave trains that are generated later lead to stress increments $\Delta\sigma_4, \Delta\sigma_5, \ldots$ Obviously the above analysis shows that the boundary condition to be imposed on the target body Ω_1 is not a constant but varies with time as a result of reflected waves coming from the interfaces. Thus the stress boundary condition at $x = 0$ comprises impact stress σ_0 (called the head wave), followed by the second wave

train $\Delta\sigma_1$ after time $t_{\sigma_1} = 2t_a$, then the third wave train $\Delta\sigma_2$ at $t_{\sigma_2} = 2t_a + 2t_b$ (if $t_a > t_b$) or at $t_{\sigma_2} = 4t_a$ (if $t_a 6 t_b$), the fourth wave train $\Delta\sigma_3$ at t_{σ_3} and so on. The exact solution should consider all these stress increments with specific time delays as the loading condition at $x = 0$. Since the formulation is linear, the late-time solution to a plate impact problem can be obtained by the method of superposition of unit step loadings with steps corresponding to incremental stress and specific time delays.

3.2.2.1. Mean stress σ_{mean}. In the present problem, the target and the impactor materials are assumed to be of infinite thickness and hence back surfaces do not exist. Waves continue to travel in the positive x-direction in the target and negative x-direction in the impactor. Waves that arrive at the plane of the impact are those that have suffered multiple interactions in the target plate. The energy content of the newly arriving waves will in general, decrease with time as more energy is being diffused away from the plane of the impact. Thus the incremental stress contribution by late arriving waves will continue to decrease and eventually vanish signalling the steady-state conditions. One can always identify a finite number n in a sequence of arriving waves such that

$$\left| \sum_{i>n}^{\infty} \Delta\sigma_i \right| < \epsilon, \tag{29}$$

where ϵ is an arbitrarily chosen, very small stress level. If this is true, then a steady-state stress value is reached at the plane of the impact (in reality throughout the domains Ω_1 and Ω_2) and this value will be designated as σ_{mean} in the present study.

In order to confirm the existence of σ_{mean} or Eq. (29), we can examine the plate impact tests of two different material systems comprising PMMA/Cu and PMMA/Al. Fig. 5(a) is the example of PMMA impacting PMMA/Cu with the thicknesses $h_1 = 0.26$ mm and $h_2 = 0.36$ mm, while Fig. 5(b) shows the stress history of aluminum impacting PMMA/Al. In both cases, the incremental stress levels in the first few steps are significantly larger than the subsequent steps and the total stress finally oscillates about a steady-stress state (marked in dotted line). The analytical results were also compared with numerical results using an explicit FEM code. FEM results (shown in thick dark lines) indicate very similar trend in the incremental stresses all the way to the steady-state. This validates the existence of σ_{mean} and possible hypothesis given in Eq. (29). Thus it is possible to use the superposition of the first few steps to obtain the value of steady-state stress σ_{mean}.

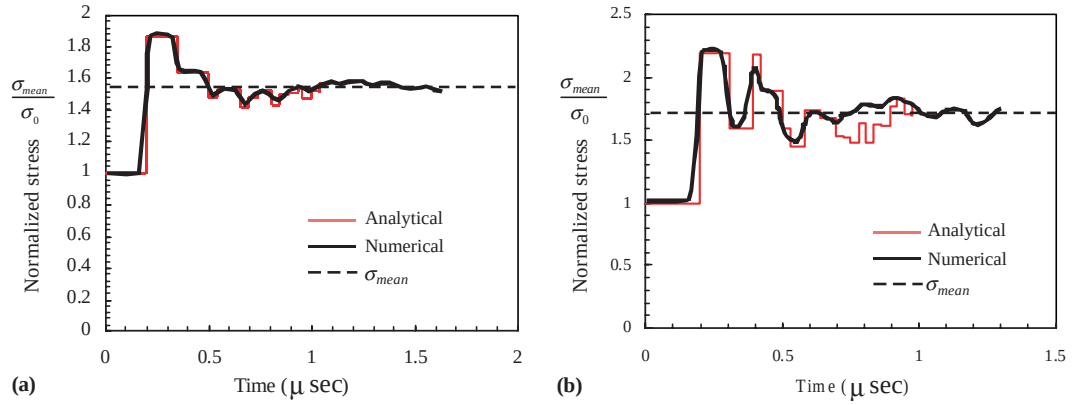

Fig. 5. Comparison of the stress history at the boundary of the layered systems between analytical solution and the numerical results: (a) PMMA impacting PMMA26/Cu36, and (b) Al impacting the PMMA26/Al36.

It should be noted that σ_0 is the stress at the instant of impact in a homogenous (as well as heterogenous) system, and is also the steady-state value for the homogenous system. For a heterogeneous system the steady-state value is σ_{mean}. The ratio $\frac{\sigma_{\text{mean}}}{\sigma_0}$ represents the amplification factor induced due to the heterogeneity of the body Ω_1. Obviously this ratio is unity if Ω_1 were to be homogeneous. Since the above procedure of computing σ_{mean} is tedious and not elegant, herein we explore other means of obtaining the same result.

The existence of the steady-state suggests rule of mixture as a possible effective medium theory. Thus invoking mixture theory, the density of the target body can be written as

$$\tilde{\rho}_0 = \eta\rho_1 + (1-\eta)\rho_2, \tag{30}$$

where η is the volume fraction of the first component (material A). For low velocity loading, we can assume that η is constant with the relation

$$\eta = \frac{h_1}{d}. \tag{31}$$

Since c_0 represents the effective sound velocity in the laminate, the equivalent impedance of the mixture is $\tilde{\rho}_0 c_0$. From the stress continuity at the impact surface, we have

$$\sigma_{\text{mean}} = \rho_3 c_3 (v_0 - u_{\text{p}}) = \tilde{\rho}_0 c_0 u_{\text{p}}, \tag{32}$$

where u_{p} is particle velocity. By eliminating u_{p}, the mean stress can be written as

$$\sigma_{\text{mean}} = \frac{\rho_3 c_3 \tilde{\rho}_0 c_0 v_0}{\rho_3 c_3 + \tilde{\rho}_0 c_0}. \tag{33}$$

From Eq. (19) and (33) we can obtain the normalized mean stress as

$$\frac{\sigma_{\text{mean}}}{\sigma_0} = \frac{\rho_3 c_3 + \rho_1 c_1}{\rho_3 c_3 + \tilde{\rho}_0 c_0} \frac{\tilde{\rho}_0 c_0}{\rho_1 c_1}. \tag{34}$$

The above relation has also been plotted in Fig. 5(a) and (b) and shows that Eq. (34) is capable of determining σ_{mean} without actually computing many incremental stress levels.

3.2.2.2. Multiple-steps loading. The determination of σ_{mean} though very useful in computing the steady-state response of heterogeneous material, still cannot capture the wave structure that precedes the steady-state value. For this we still need to use multiple steps as outlined below. We can now propose a solution that comprises n steps in the stress loading function at the plane of impact due to first n wave trains. In order to make the final steady-state reach σ_{mean}, we set

$$\Delta\sigma_{n-1} = \sigma_{\text{mean}} - \sigma_{n-2}. \tag{35}$$

For example, for a four-step method (when $n = 4$), the fourth step is specified by

$$\Delta\sigma_3 = \sigma_{\text{mean}} - \sigma_2. \tag{36}$$

The whole loading history at the impact plane is shown in Fig. 4(b). Now we consider each step as a case of unit step loading with its amplitude and starting time determined by the scattering process. Through superposition, the solution can be written as

$$\sigma(x,t) = \begin{cases} \sigma_0(x,t), & \frac{x}{c_0} \leqslant t < t_{\sigma_1} + \frac{x}{c_0}, \\ \sigma_0(x,t) + \Delta\sigma_1(x,t), & t_{\sigma_1} + \frac{x}{c_0} \leqslant t \leqslant t_{\sigma_2} + \frac{x}{c_0}, \\ \sigma_0(x,t) + \Delta\sigma_1(x,t) + \Delta\sigma_2(x,t), & t_{\sigma_2} + \frac{x}{c_0} < t < t_{\sigma_3} + \frac{x}{c_0}, \\ \sigma_0(x,t) + \Delta\sigma_1(x,t) + \Delta\sigma_2(x,t) + \Delta\sigma_3(x,t), & t_{\sigma_3} + \frac{x}{c_0} < t, \end{cases} \tag{37}$$

where

$$\sigma_0(x,t) = \sigma_0\left[\frac{1}{3} + \int_0^B Ai(-s)\,ds\right],$$

and

$$\Delta\sigma_j(x,t) = \Delta\sigma_j\left[\frac{1}{3} + \int_0^B Ai(-s)\,ds\right], \quad j = 1,2,3,4. \tag{38}$$

The above equations can be solved similar to Eqs. (16)–(18) (see also Appendix A, (A.24)–(A.26)). The solution so obtained is usually referred to as the *late-time solution*. Late-time solution should rather be called as far-field solution and should be distinguished from steady-state solution as discussed below.

3.2.2.3. Application of the late-time solution based on elastic analysis. As shown in Section 3.2.1, the late-time solution predicts the stress history at a far-field arising from the contribution of the main disturbance, when the frequency $s \to 0$. Theoretically, the late-time solution is only valid when $t \to \infty$ and $x \to \infty$. However, in order to use the analytical solution in practical problems, one would like to identify a distance $x > x^*$ for which the solution is reasonably valid. If we decompose the incident square wave into Fourier series, the coefficients of the terms with higher frequencies are increasingly smaller. Also, dispersion relation given by Eq. (10) indicates that the higher the frequency, the lower the phase velocities (Bedford and Drumheller, 1994). Thus the effect of low frequency predominates at a large x distance over the high frequency content, and hence the latter can be neglected in preference to the former. Thus for sufficiently large x, the head of the pulse can be approximated by Eq. (16). Based on the high frequency concept discussed above, we can identify the location x^* where the head wave dies out. Here, we refer to head wave as the first wave travelling in the heterogeneous medium with successive transmissions. Thus for location $x \geqslant x^*$ late-time solutions presented in this paper can be used. For $x < x^*$, we need to consider the effect of all the interacting waves as discussed in our earlier paper (Chandra et al., 2002). Additionally, from the hypothesis of x^*, it is clear that x^* in a system with high impedance mismatch (equivalent to high $r_{A\text{–}B}$), is much smaller than that in another system with small $r_{A\text{–}B}$, if their geometric parameters are the same.

Having determined the region where late-time solution is valid ($x \geqslant x^*$), it then becomes important to find out how many steps n are required for obtaining the stress response with a specified level of accuracy. At a fixed location, our numerical study shows that the accuracy depends on $|\sum_{i>n}^{\infty} \Delta\sigma_i|$, which in turn is affected by material heterogeneity. One measure of heterogeneity factor is impedance mismatch. It is found that systems with very high impedance mismatch between materials A and B within the target (high $r_{A\text{–}B}$) yield small $|\sum_{i>n}^{\infty} \Delta\sigma_i|$. For systems with high $r_{A\text{–}B}$, one step ($n = 1$) solution seems to produce acceptable result. In the case the equivalent loading condition is given by

$$\sigma(0,t) = \sigma_{\text{mean}} H(t). \tag{39}$$

In the above equation it is implied that σ_{mean} is applied at $t = 0$ rather than the impact stress, σ_0. In truth σ_{mean} is reached at time $t > 0$, and this effect of time is ignored by Eq. (39). For cases with high $r_{A\text{–}B}$, this assumption implies that the time to reach σ_{mean} is small which is understandable. Thus for cases with high $r_{A\text{–}B}$ we can substitute σ_0 by σ_{mean} in Eq. (16) to obtain the solution for plate impact as

$$\sigma(x,t) = \sigma_{\text{mean}}\left[\frac{1}{3}\int_0^B Ai(-s)\,ds\right]. \tag{40}$$

In order to validate the above ideas, we select PMMA/Al system with a high impedance ratio of $r_{A\text{–}B} = 0.71$ and examine the effect of number of loading steps n on the accuracy of the solution. Fig. 6 shows the stress response at $x = 10$ mm (impact conditions identical to that in Fig. 5(b)), using 1, 3 and 5 steps. Numerical results using an explicit finite element code is also presented for comparison purposes. Fig. 6 clearly shows

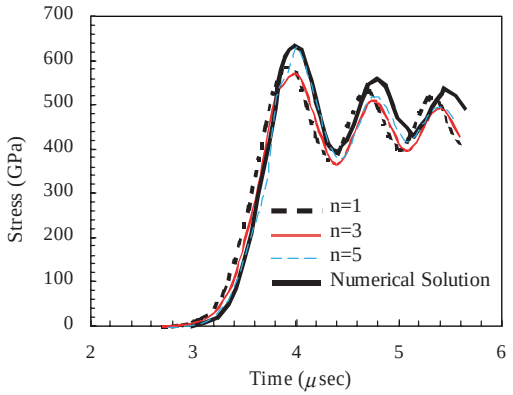

Fig. 6. Comparison of solution for Al impacting PMMA26/Al36 at $x = 10$ mm. Comparison between FEM result and analytical solution using $n = 1, 3, 5$, respectively.

that one step solution gives sufficiently accurate results for this case. Though the results are not shown here, when impedance ratio r_{A-B} is small (for example, below 0.4), the use of one-step method may not be sufficient and higher number of steps are needed.

All the analyses presented so far, assume that the impact process generates a single elastic wave that travels away from the impact plane. When velocity of impact increases, the wave enters an elastic–plastic regime and with further increase the wave becomes a shock wave. For both these cases, the approaches presented above need to be modified. For the case of shock wave, we present the necessary modifications in the next section.

3.2.3. *Approximate solution for shock loading*

The solution given in Section 3.2.2 assumes that the constituent layers are linear elastic and isotropic. When the loading strength is much higher than the Hugoniot Elastic Limit (HEL), shock waves are generated. Shock response of materials is a highly nonlinear process and is extremely difficult if not impossible to obtain purely analytical solutions. However, an approximate explicit solution based on the previously developed elastic solution can be obtained for shock loading cases by invoking hydrodynamic treatment ignoring shear stresses. It is important to note that we are dealing with shock response and not the elastic–plastic response which is of two-wave structure. In shock loading cases, stress non-linearity depends on the strain. And the slope of the conventional pressure-particle velocity plot represents shock impedance. We extend the elastic analysis to shock response by incorporating the non-linear effects through computing shock velocities of the wave trains and superimposing them. Even though the material response of the constituents is different in shock regime, the structural response of the laminate remains similar to the elastic regime. For example, both elastic and shock waves are of one-wave structures. Also, the wave scattering processes at interfaces are similar following the rules of reflection and transmission. Most importantly, it can be seen from previous experiments (Section 2) that an approximate steady-state can also be reached in a given layered system. This can be partly explained by the fact that the cumulative amplitude of the waves remains unchanged during multiple wave interactions or during reflections at interfaces.

For laminated systems under shock loading, velocities of the shock waves depend on the pressure. Therefore, it is necessary to relate shock velocity, density and volume to the particle velocity by means of equation of state (EOS) (Meyers, 1994). A general EOS takes the form

$$U_s = C_0 + S_1 u_p + S_2 u_p^2 + S_3 u_p^3 + \cdots, \tag{41}$$

where S_1, S_2 and S_3 are empirical parameters. C_0 is the sound velocity in a given material under zero pressure. For most metals (without porosity and phase transformation), linear relationship between U_s and u_p is sufficiently accurate and EOS assumes the form

$$U_s = C_0 + S_1 u_p. \tag{42}$$

For materials other than metals, such as polymers, higher order terms need to be included in the EOS. The density under high pressure (ρ_i') can no longer be approximated as the original density. It is directly related to the loading strength represented by particle velocity u_{pi} with

$$\rho_i' = \frac{1}{1 - \frac{u_{pi}}{U_{si}}} \rho_i, \quad i = 1, 2, 3. \tag{43}$$

In the same way, the volume under high pressure (V_i') is related to u_{pi} by

$$V_i' = \left(1 - \frac{u_{pi}}{U_{si}}\right) V_i, \quad i = 1, 2, 3. \tag{44}$$

Therefore, in plate impact problem, according to the above equation, the thickness under shock loading condition (h_i') will be

$$h_i' = \left(1 - \frac{u_{pi}}{U_{si}}\right) h_i, \quad i = 1, 2. \tag{45}$$

New impedance ratio is approximately (assuming that material 2 is harder than material 1)

$$R' = \frac{\rho_2' U_{s2}}{\rho_1' U_{s1}}. \tag{46}$$

It can be seen from Eqs. (41), (42), (43) and (45) that wave velocity, thickness and density for the laminates subjected to shock loading, all depend on the particle velocity, while they remain constant for elastic response. Though velocity is not continuous across a strong shock front, it can be assumed to be continuous for shocks with moderate amplitude which is the case considered here. Therefore, by substituting the U_{si}, ρ_i' and h_i' $(i = 1, 2)$ into Eq. (11), we obtain the late-time velocity for shock loading condition $(\tilde{U}_s)$ as

$$\tilde{U}_s = \frac{h_1' + h_2'}{\left[\left(\frac{h_1^0}{U_{s2}}\right)^2 + \left(\frac{h_2^0}{U_{s2}}\right)^2 + \left(R' + \frac{1}{R^0}\right)\frac{h_1^0 h_2^0}{U_{s1} U_{s2}}\right]^{1/2}}. \tag{47}$$

Similarly, we obtain the mean stress level for a layered system (σ_{mean}') by assuming that this layered system is equivalent to a mixture with impedance $\tilde{\rho}_0 \tilde{U}_s$. Similar to Eqs. (32) and (33), we have

$$\sigma_{mean}' = \tilde{\rho}_0 \tilde{U}_s \tilde{u}_p' = \frac{\tilde{\rho}_0 \tilde{U}_s \rho_3 U_{s3}}{\rho_3 U_3 + \tilde{\rho}_0 \tilde{U}_s} v_0. \tag{48}$$

Thus we have obtained σ_{mean}' (Eq. (48)), the steady-state stress value for shock loading conditions analogous to σ_{mean} for elastic loading. However, we need to be very cautious in selecting the number of steps (or wave trains) since in shock loading conditions different wave trains travel with different velocities. It is possible that a wave train can travel faster than its predecessor and may even overtake it. This phenomenon in shock loading conditions may dictate the use of more steps for capturing this effect.

For an observer at a given location, the head wave propagates with longitudinal velocity into uncompressed media. So for a given location $x(x = Ld)$, the arrival time of the head wave is

$$t_{\sigma_o^0} = \sum_{j=1}^{L} \frac{\eta d}{(U_{s1})_j} + \frac{(1-\eta)d}{(U_{s2})_j}, \tag{49}$$

where $(U_{s1})_j$, $(U_{s2})_j$, are the sound velocities of waves in previously uncompressed materials A and B within jth unit cell, and η is given by Eq. (31). Immediately behind the head wave, the high pressure σ_0' is achieved

$$\sigma_0' = \frac{\rho_3 U_{s3} \rho_1 U_{s1} v_0}{\rho_3 U_{s3} + \rho_1 U_{s1}}. \tag{50}$$

Thus the second wave train can travel faster than the head wave since the material is highly compressed given by Eq. (50). As shown in Fig. 4(a), the second wave train is generated by one reflection inside first layer (in Material A), and reaches the impact surface after $\Delta t'$ from initial impact:

$$\Delta t' = \frac{h_1}{U_{s1}} + \frac{h_1'}{U_{11}}, \tag{51}$$

where U_{11} is the wave velocity in material A in compressed media after the wave reflection in the first A–B interface. For a soft to hard arrangement in the target plate ($\rho_1 c_1 < \rho_2 c_2$), the pressure in the first layer increases after the reflection, so we have $U_{11} > U_{s1}$. Similarly, the second wave train will travel faster than the head wave in other layers. As shown in Eq. (51), the time interval between the second wave train and the head wave is determined by the thickness and wave velocity of the first layer before and after the arrival of the head wave. The time $t_{\sigma_1^0}$ when the second wave train arrives at location x is given by

$$t_{\sigma_1^0} = \Delta t' + \sum_{j=1}^{L} \left(\frac{\eta d}{(U_{s1})_{j,\sigma_o^0}} + \frac{(1-\eta)d}{((U_{s2})_{j,\sigma_o^0})} \right), \tag{52}$$

where $(U_{s1})_{j,\sigma_o^0}$ and $(U_{s2})_{j,\sigma_o^0}$ represent the shock velocities in materials A and B in jth unit after initial compression, respectively. The propagation distance x where the second wave catches up with the head wave depends on head wave velocity, time of origin of second wave and the compressive stress in the media as given by Eqs. (52) and (49). As a matter of fact, it can be shown that this 'overtaking' effect is critical for capturing the peak stress in shock wave regime.

Thus the steps in the analytical procedure for determining the stress response under shock loading conditions are as follows:

1. The shock velocities U_{si}, and the thickness h_i' should be calculated by considering EOS, as shown in Eqs. (41)–(45).
2. The mean stress σ'_{mean} should be computed using Eqs. (47) and (48).
3. Incident stress in the shock regime σ_0' is given by Eq. (50). Incremental stress values at the impact plane $\Delta\sigma_0', \Delta\sigma_1', \ldots$ should be calculated using σ_0' in Eqs. (21) and (23), unless modification of reflection ratio is needed based on velocity variation with pressure.
4. The number of steps, n should be carefully chosen depending on the location x for which the stress is computed, n should be at least equal to the number of steps needed to reach the first peak from σ_0' at the impact plane.
5. The effect of 'overtaking' of a successor wave over a predecessor wave should be evaluated by comparing Eqs. (49) and (51). When overtaking takes place, the time interval between these two waves are set to zero in Eq. (37).

3.3. Modeling plate impact experiments

We first demonstrate the need to use σ_{mean} for solving plate impact problems rather than σ_0, the stress at the impact plane at the time of the impact. It is also shown that the ratio $\frac{\sigma_{mean}}{\sigma_0}$ can be quite high and depends

on a number of heterogeneity factors including the volume fraction of each constituent, the material of the impactor, and the velocity of impact. In the next section, we examine the shock velocities of each of the material in the layered system and how they affect the effective shock wave velocity. It is then shown that the effective material heterogeneity depends on the combination of the materials that comprise the layered system. Here, we apply the developed method to simulate plate impact tests corresponding to the test configuration used by Zhuang (2002). In the first experiment, a flyer made of polycarbonate (PC) impacts on a target made of alternating PC and glass (GS) with velocity of 1079 m/s, as shown in Table 2. The thickness of the PC and GS layers are 0.37 and 0.20 mm, respectively. In the second test, also shown in Table 2, a metallic impactor (aluminum) impacts the same composite system with an impact velocity of 1160 m/s. The comparisons of the experimental data and the analytical solutions are given in Fig. 7. It is clearly seen that very good agreement has been obtained between these two results by matching the detailed structure.

3.3.1. Mean stress σ_{mean}

When a heterogeneous target material (see Sections 3.2) is subjected to plate impact test, σ_{mean} is the steady-state stress. In some sense $\frac{\sigma_{\text{mean}}}{\sigma_0}$ represents the heterogeneity of the target system. The heterogeneity effect given by Eq. (34) is plotted in Fig. 8, which shows the magnitude of $\frac{\sigma_{\text{mean}}}{\sigma_0}$ for PMMA (matrix) based composites systems. Various polymer and metallic materials are used to reinforce the composites. The figure shows the variation of $\frac{\sigma_{\text{mean}}}{\sigma_0}$ with varying volume fraction of PMMA in the composites. Two sets of data are shown in the figure: the data in the solid line are for cases when the flyer plate is PMMA, while the data in the dashed lines are for the cases when the flyer plate is aluminum. It can be seen from the figure that $\frac{\sigma_{\text{mean}}}{\sigma_0}$ can vary from 0.9 to 4.8. It should be noted that the maximum values of $\frac{\sigma_{\text{mean}}}{\sigma_0}$ shown in this plot assumes

Table 2
Configurations of Experiments 1 and 2 (Zhuang, 2002)

Experiments	A	B	C	Impact velocity (m/s)	h_1 (mm)	h_2 (mm)	Gauge location x
1	PC	Glass	PC	1079	0.37	0.20	6.44
2	PC	Glass	Al	1160	0.37	0.20	3.55

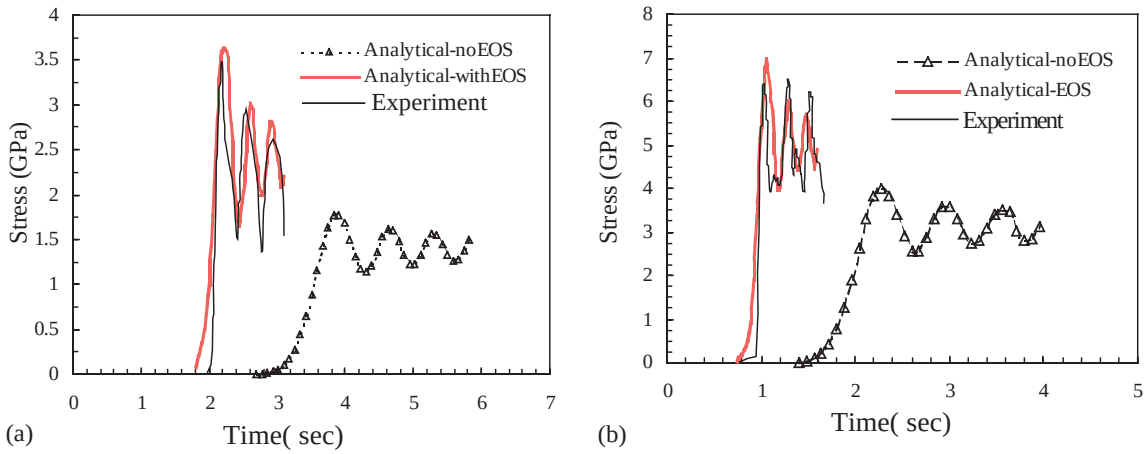

Fig. 7. Comparisons of the experimental data and the analytical solutions in layered PC/GS: (a) Experiment 1 and (b) Experiment 2 (Zhuang, 2002).

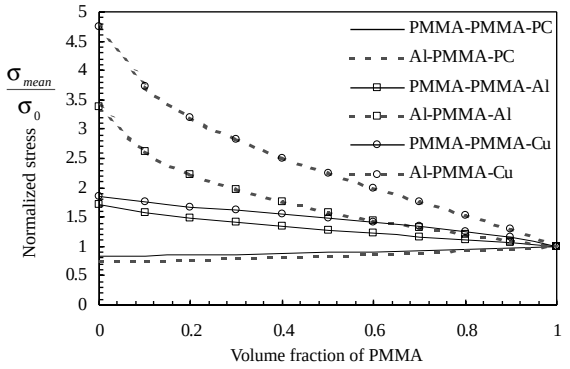

Fig. 8. The normalized mean stress as a function of volume fraction in different systems.

the volume fraction of PMMA cannot be zero. $\frac{\sigma_{\text{mean}}}{\sigma_0}$ ratio represents the amplification in the stress levels reached within the material compared to that at the time of impact, and the figure shows that the ratio can be very high. Since this ratio can be very high, it clearly demonstrates that only σ_{mean} should be used to model the steady-state response of a plate impact problem. It should be noted that while σ_0 is dictated by the heterogeneity at the impact surface (materials A and C) and of course the impact velocity, the magnitude of σ_{mean} depends additionally on the impedance mismatch of the components of the target materials (A and B) and their volume fraction.

Since the magnitude of σ_{mean} uniquely determines the steady-state stress in the materials subjected to plate impact loading, it is interesting to explore whether other theories can lead to the same result. For this purpose we examine Dremin's mixture theory. As shown in Appendix B, the same effective sound speed for the equivalent mixture can be obtained based on this theory. So by obtaining the same effective density and sound velocity in the mixture, the same expression of mean stress can be obtained by applying Eqs. (32) and (33). However, as mentioned in Section 2, except for the value of mean stress, mixture theory cannot predict the complete structure.

3.3.2. The effect of equation of state

When velocity of impact is high enough to generate shock waves, then we need to use equation of state (EOS). When the target plate is made up of multiple materials with their individual EOS, the application of EOS of the system is not straightforward. EOS can be expressed as a variation of shock velocity with particle velocity. Fig. 9(a) shows shock velocity, U_s as a function of particle velocity, u_p for a few materials of interest. The slope of the curve $\frac{\partial U_s}{\partial u_p}$ is different for different materials; typically the slope varies linearly for metals and nonlinearly for polymers. Thus the parameter S_1 in Eq. (42) determines the slope for metals. While S_1 plays a major role, S_2 and S_3 or even higher orders cannot be neglected for polymers. It is clear from this figure that the slope $\frac{\partial U_s}{\partial u_p}$ increases the fastest for polycarbonate (PC) while there is negligible slope for glass. The slopes of Cu, Al and PMMA show only moderate values.

It should be noted that the impedance mismatch for a pair of given materials not only depends on the relative magnitudes of shock velocities but on the densities at a given state. For materials under shock loading conditions, apart from the velocities there is a concurrent increase in densities with particle velocity. Since impedance is the product of density and shock velocity, and since both increase with particle velocity, absolute value of the impedance of a given material increases. However, since $\frac{\partial U_s}{\partial u_p}$ and the rate of density change is different for different materials, impedance mismatch of a given pair materials may increase or decrease. Fig. 9(b) shows the impedance *mismatch* of combinations of materials (described in Fig. 9(a)) with particle velocities. It can be clearly seen from the figure that the impedance mismatch is not a constant for a

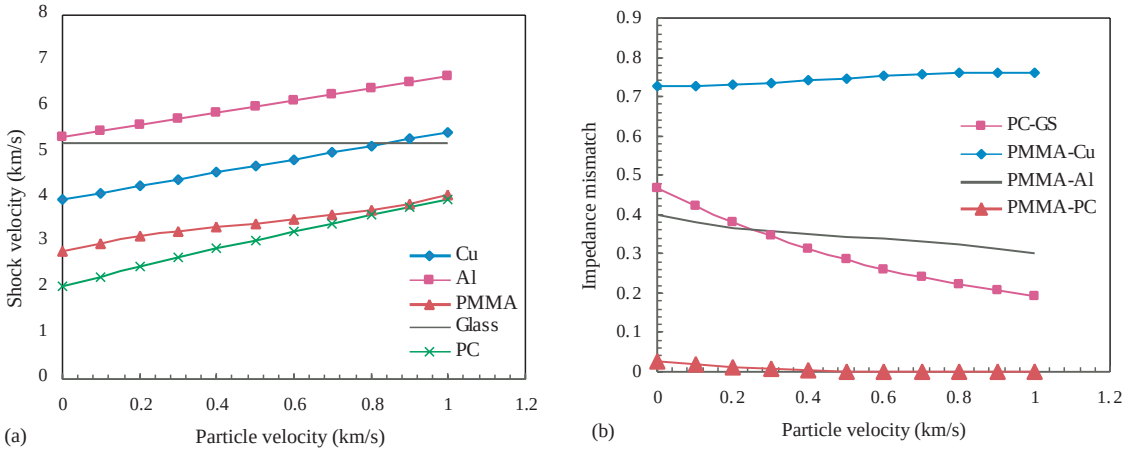

Fig. 9. The effect of EOS on velocity and impedance mismatch.

given material combination but is a function of particle velocity and hence the velocity of impact. For example, the impedance of PC-GS reduces significantly with the increase in particle velocity. However, for other systems considered here the variation is less significant.

It can be seen from Fig. 7 that the mean stress obtained from analytical solution agrees well with the experimental results for both cases. It should be noted that by incorporating EOS, the shock velocity and the density generally increase depending on the loading strength. As a result, the mean stress level obtained based on Section 3.2.3 can be significantly higher than the mean stress obtained using just elastic analysis (showed in dotted line). The elastic solution does not even come close to the experimental results clearly emphasizing the need to use EOS. There is yet another critical difference between elastic and shock loading conditions in terms of the peak stress. In the elastically loaded condition, the first peak has a magnitude of 1.274 σ_{mean} when the steady-state stress is σ_{mean}, while this is not true for shock loading. It is important to note that peak stress may be more critical than mean stress in determining the fracture or damage of materials. Fig. 7(a) and (b) shows that the first peak stress in both the cases are much higher than 1.274 σ_{mean}. This anomaly can be explained by the fact that wave trains in compressed media travel faster and the second wave may be able to overtake the first wave depending on the distance of propagation, as discussed earlier. Thus using a single step method may not be adequate for shock loaded cases while it may be acceptable for elastic loadings. The matching of experimental and analytical results is quite good, in terms of arrival time, peak stress, frequency of the oscillations, and mean stress.

4. Summary

In this paper, an analytical solution to the problem of plate impact in layered heterogeneous material systems has been developed. The plate impact problem (Fig. 2(c)) has been clearly shown to be quite different from the problem of unit step loading. The stress boundary condition in a plate impact test of a heterogeneous layered target at the plane of the impact continuously varies due to multiple wave interactions inside the target plate. The work can be briefly summarized as follows.

- A steady-state stress value, σ_{mean}, has been identified for the case of heterogeneous target system. This σ_{mean} is different from the value at the time of impact σ_0, and the difference depends on the degree of material heterogeneity.

- The ratio $\frac{\sigma_{\text{mean}}}{\sigma_0}$ can be quite high and depends on the volume fraction of constituents, material of the flyer plate and the velocity of impact among others.
- The magnitude of σ_{mean} has been determined using wave dispersion relation. It was further shown that the same relationship can also be alternatively obtained using Dremin's mixture theory.
- A late-time solution to the problem of plate impact on a heterogeneous layered material system has been developed. The spatial range for which the late-time solution is valid ($x > x^*$) has been identified.
- The solution procedure for elastic loading has been formulated using multiple steps. The conditions for using a single step method have also been identified.
- The solution method for shock loaded cases has also been outlined.
- The developed method has been validated by comparing the analytical results with numerical and experimental data. The comparison is very good.

Appendix A. The late-time solution for unit step loading

Take Laplace transform of Eqs. (1)–(3)

$$\frac{\partial \bar{\sigma}(x,s)}{\partial x} = \rho_i s \bar{v}(x,s), \tag{A.1}$$

$$\frac{\partial \bar{v}(x,s)}{\partial x} = -s\bar{\varepsilon}(x,s) = 0, \tag{A.2}$$

$$\bar{\sigma}(x,s) = E_i^{\text{e}} \bar{\varepsilon}(x,s). \tag{A.3}$$

The solution of equations of Eqs. (A.1)–(A.3) are in the form

$$\bar{v}(x,s) = a_i \mathrm{e}^{k_i x} + b_i \mathrm{e}^{-k_i x}, \tag{A.4}$$

$$\bar{\sigma}(x,s) = a_i \left(\frac{s\rho_i}{k_i} \right) \mathrm{e}^{k_i x} + b_i \left(-\frac{s\rho_i}{k_i} \right) \mathrm{e}^{-k_i x}, \tag{A.5}$$

where

$$k_i = k_i(s) = \frac{s}{c_i} \tag{A.6}$$

and c_i is phase velocity given by

$$c_i = \left[\frac{E_i^{\text{e}}}{\rho_i} \right]^{1/2}.$$

For ordinary differential equations with periodic coefficients, Floquet theory can be applied

$$\bar{\sigma}(x,s) = \mathrm{e}^{k(s)d} \bar{\sigma}(x-d,s), \tag{A.7}$$

$$\bar{v}(x,s) = \mathrm{e}^{k(s)d} \bar{v}(x-d,s). \tag{A.8}$$

By considering the stress and velocity continuity across $x = h_1$, let $L = 0$ in Eqs. (6) and (8), then

$$a_1 \mathrm{e}^{k_1 h_1} + b_1 \mathrm{e}^{-k_1 h_1} = a_2 \mathrm{e}^{k_2 h_1} + b_2 \mathrm{e}^{-k_2 h_1}, \tag{A.9}$$

$$a_1 \left(\frac{\rho_1}{k_1} \right) \mathrm{e}^{k_1 h_1} - b_1 \left(\frac{\rho_1}{k_1} \right) \mathrm{e}^{-k_1 h_1} = a_2 \left(\frac{\rho_2}{k_2} \right) \mathrm{e}^{k_2 h_1} - b_2 \left(\frac{\rho_2}{k_2} \right) \mathrm{e}^{-k_2 h_1}. \tag{A.10}$$

Stress and velocity continuity across $x = d$

$$e^{kd}(a_1 + b_1) = a_2 e^{k_2 d} + b_2 e^{-k_2 d}, \tag{A.11}$$

$$e^{kd}\left(a_1 \frac{\rho_1}{k_1} - b_1 \frac{\rho_1}{k_1}\right) = a_2 \frac{\rho_2}{k_2} e^{k_2 d} - b_2 \frac{\rho_2}{k_2} e^{-k_2 d}. \tag{A.12}$$

Eqs. (A.9)–(A.12) have non-trivial solutions only when the determinant of the coefficients is equal to zero. This condition yields the transcendental dispersion relation

$$\cosh kd = \cosh k_1 h_1 \cosh k_2 h_2 + \frac{1}{2}\left(\frac{\rho_1 c_1}{\rho_2 c_2} + \frac{\rho_2 c_2}{\rho_1 c_1}\right) \sinh k_1 h_1 \sinh k_2 h_2. \tag{A.13}$$

where k is wave number for the laminates, k_1 and k_2 are frequencies for layer A and layer B, where h_1, h_2 and c_1, c_2 are the thickness and the longitudinal wave velocities of the layers respectively. And d is the thickness of the unit cell, with $d = h_1 + h_2$, as shown in Fig. 2(c).

For steady wave with frequency s, the dispersion relation can be written as

$$\cosh kd = \cosh \frac{s}{c_1} h_1 \cosh \frac{s}{c_2} h_2 + \frac{1}{2}\left(\frac{\rho_1 c_1}{\rho_2 c_2} + \frac{\rho_2 c_2}{\rho_1 c_1}\right) \sinh \frac{s}{c_1} h_1 \sinh \frac{s}{c_2} h_2. \tag{A.14}$$

Therefore, the phase velocity for zero-frequency limit c_0 is obtained

$$c_0 = \frac{d}{\left\{\left(\frac{h_1}{c_1}\right)^2 + \left(\frac{h_2}{c_2}\right)^2 + \left(\frac{\rho_1 c_1}{\rho_2 c_2} + \frac{\rho_2 c_2}{\rho_1 c_1}\right)\frac{h_1 h_2}{c_1 c_2}\right\}^{1/2}}. \tag{A.15}$$

In order to get the solution for plate impact loading, it is convenient and necessary to show the solution for the problem of unit step loading. For unit step loading, the boundary condition for the target plate can be written as

$$\sigma(0, t) = \sigma_0 H(t). \tag{A.16}$$

Its corresponding Laplace transform is

$$\sigma(0, s) = \frac{\sigma_0}{s}. \tag{A.17}$$

The transformed stress at distance $x = Ld$ can be obtained by Floquet theory

$$\sigma(Ld, s) = e^{k(s)Ld/2} \frac{\sigma_0}{s} \tag{A.18}$$

The late-time solution can be obtained by the asymptotic evaluation of the integral

$$\sigma(Ld, t) = \frac{1}{2\pi i} \int_{\gamma - i\infty}^{\gamma + i\infty} \bar{\sigma}(2Ld, s) e^{st}\, ds. \tag{A.19}$$

Now introduce a small time scale

$$\delta = t - x/c_0. \tag{A.20}$$

By introducing δ, we remove the variable x in the stress function in Eq. (A.19). Substitute Eqs. (A.20) and (A.18) to Eq. (A.19) and assume $p(t, \delta)$ is the stress function with t and δ being the variables,

$$p(t, \delta) = \frac{\sigma_0}{2\pi i} \int_{\gamma - i\infty}^{\gamma + i\infty} \frac{e^{-\delta g(s)} e^{th(s)}\, ds}{s}, \tag{A.21}$$

where

$$g(s) = k(s)c_0,$$

$$h(s) = g(s) + s = k(s)c_0 + s.$$

For late-time solution, we seek an asymptotic representation of $p(t,\delta)$ for $t \to \infty$ with fixed δ. Such representation can be obtained by making the integration path follows a path of steepest descent though the saddle point s_0 at which $h'(s) = 0$. This happens when $s \to 0$. The expansion of about the saddle point yields (for elastic cases)

$$h(s) = \frac{h'''(0)}{3!}s^3, \tag{A.22}$$

where

$$h'''(0) = \frac{(c_0)^2}{d^2}\left\{\left(\frac{h_1}{c_1}\right)^2\left(\frac{h_2}{c_2}\right)^2\left[\frac{1}{4}\left(\frac{\rho_1 c_1}{\rho_2 c_2} + \frac{\rho_2 c_2}{\rho_1 c_1}\right)^2 - 1\right]\right\}. \tag{A.23}$$

So the integral of Eq. (A.21) becomes

$$p(t,\delta) = \frac{1}{3}\sigma_0 + \frac{\sigma_0}{2\pi \mathrm{i}}\int_\Gamma \frac{\mathrm{e}^{\delta s\frac{h^{000}(0)}{3!}s^3}}{s}\,\mathrm{d}s. \tag{A.24}$$

Evaluation of the integral in Eq. (A.24) will finally give an integral of the Airy function.

$$\sigma(x_{Ld},t) = \sigma_0\left[\frac{1}{3} + \int_0^B A\mathrm{i}(-s)\,\mathrm{d}s\right], \tag{A.25}$$

where

$$B = \left(t - \frac{x}{c_0}\right)\left(\frac{2}{h'''(0)t}\right)^{1/3}. \tag{A.26}$$

The above solution for unit step loading follows Chen and Clifton's (1975) work. Also, it should be noted that Sve (1972) evaluated an integral analogous to Eq. (A.21) and obtained the same final result.

Appendix B. Dremin's theory in finding effective wave speed

In this theory, it is assumed that the specific volume of the shock-compressed mixture is equal to the sum of the specific volume of its components, obtained at the same pressure by separate shock compression

$$\tilde{V} = \alpha V_1(P) + (1-\alpha)V_2(P), \tag{B.1}$$

where P is the pressure or stress, $\tilde{V}$,V_1 and V_2 are the specific volumes of the mixture, materials 1 and 2, respectively. α is the mass fraction of component 1. Differentiating the above equation with respect to pressure P, we obtain

$$\frac{\mathrm{d}\tilde{V}}{\mathrm{d}P} = \alpha\frac{\mathrm{d}V_1}{\mathrm{d}P} + (1-\alpha)\frac{\mathrm{d}V_2}{\mathrm{d}P}. \tag{B.2}$$

In the above equation $\frac{d\tilde{V}}{dP}$ represents the slope of Hugoniot curve of the mixture which can then be equated as follows:

$$\frac{d\tilde{V}}{dP} = -\frac{\tilde{V}^2}{\tilde{U}_s^2}. \tag{B.3}$$

The above Eq. (B.3) can be written for each of the constituent materials 1 and 2, and that of the mixture. Now using those definitions in Eq. (B.2) we obtain the shock velocity $\tilde{U}_s$ of the mixture

$$\tilde{U}_s = \frac{\tilde{V}}{\left[\frac{\alpha}{(\rho_s U_{s1})^2} + \frac{(1-\alpha)}{(\rho_2 U_{s2})^2}\right]^{1/2}}. \tag{B.4}$$

In elastic region, the effective volume in the above equation is given by

$$\tilde{V} = \frac{1}{\tilde{\rho}_0} = \frac{h_1 + h_2}{\rho_1 h_1 + \rho_2 h_2}. \tag{B.5}$$

Also, conservation of mass holds for each constituent as well as for the mixture, so the mass fraction of the material 1 is given by $\alpha = \frac{\rho_1 h_1}{\rho_1 h_1 + \rho_2 h_2}$. By substituting α and the specific volume $\tilde{V}$ in Eq. (B.5) into Eq. (B.4), we have

$$\tilde{U}_s = \frac{h_1 + h_2}{\left[(\rho_1 h_1 + \rho_2 h_2)\left(\frac{\rho_1 h_1}{\rho_1^2 c_1^2} + \frac{\rho_2 h_2}{\rho_2^2 c_2^2}\right)\right]^{1/2}}. \tag{B.6}$$

By expansion of the terms in the denominator and rearrangement of these terms, it is found that

$$\tilde{U}_s = \frac{h_1 + h_2}{\left[\left(\frac{h_1}{c_1}\right)^2 + \left(\frac{h_2}{c_2}\right)^2 + \left(\frac{\rho_1 c_1}{\rho_2 c_2} + \frac{\rho_2 c_2}{\rho_1 c_1}\right)\frac{h_1 h_2}{c_1 c_2}\right]^{1/2}} = c_0. \tag{B.7}$$

In the same manner, it can be shown that under shock loading condition the same velocity is also obtained through these two different theories.

References

Barker, L.M., 1971. A model for stress wave propagation in composite materials. Journal of Composite Materials 5, 140–162.

Barker, L.M., Lundergan, C.D., Chen, P.J., Gurtin, M.E., 1974. Nonlinear viscoelasticity and the evolution of stress waves in laminated composites: A comparison of theory and experiment. Journal of Applied Mechanics, 1025–1030.

Bedford, A., Drumheller, D.S., 1994. Introduction to elastic wave propagation. Wiley, New York.

Boteler, J., Rajendran, A.M., Grove, D., 1999. Shock wave profile in polymer matrix composite. Shock Compression of Condensed Matter, 563–566.

Chandra, N., Chen, X., Rajendran, A.M., 2002. The effect of material heterogeneity on the shock response of layered systems in plate impact tests. Journal of Composite Technology and Research 24 (4), 232–238.

Chen, C.C., Clifton, R.J., 1975. Asymptotic solutions for wave propagation in elastic and viscoelastic bilaminates. In: Proceedings of the 14th Midwestern Mechanics Conference, University of Oklahoma, Developments in mechanics, vol. 8, pp. 399–417.

Clements, B.E., Johnson, J.N., Hixson, R.S., 1996. Stress waves in composite materials. Physics Review E 54, 6876–6888.

Dandekar, D., Beaulieu, P.A., 1995. Shots 518 and 521-1. In: AMD, vol. 48. ASME, New York. pp. 63–70.

Espinosa, H.D., Dwivedi, S., Lu, H.C., 2000. Modeling impact induced delamination of woven fiber reinforced composites with contact/cohesive laws. Computer Methods in Applied Mechanics and Engineering. 183 (3–4), 259–290.

Floquet, G., 1880. Sur les équations différentielles linéaires á coefficients périodiques. C.R. Acad. Sci. Paris 91, 880–882.

Kanel, G.I., Ivanov, M.F., Parshikov, A.N., 1995. Computer simulation of the heterogeneous materials response to the impact loading. International Journal of Impact Engineering 17, 455–464.

Lundergan, C.D., Drumheller, D.S., 1971. Propagation of stress waves in a laminated plate composite. Journal of Applied Physics 42 (2), 669–675.

Meyers, M.A., 1994. Dynamic Behavior of Materials. Wiley, New York.

Nesterenko, V.F., 2001. Dynamics of Heterogeneous Materials. Springer, New York.

Oved, Y., Luttwak, G.E., Rosenberg, Z., 1978. Shock wave propagation in layered composites. Journal of Composite Materials 12, 84–89.

Peck, J.C., Gurtman, G.A., 1969. Dispersive pulse propagation parallel to the interfaces of a laminated composite. Journal of Applied Mechanics 36, 479–484.

Rytov, S.M., 1956. Acoustic properties of a thiny laminated medium. Soviet Physics Acoustics 2, 68–80.

Sun, C.T., Achenbach, J.D., Herrmann, G., 1968. Continuum theory for a laminated medium. Journal of Applied Mechanics 35, 467–475.

Sve, 1972. Stress wave attenuation in composite materials. Journal of Applied Mechanics 39, 1151–1153.

Ting, T.C.T., 1980. The effects of dispersion and dissipation on wave-propagation in viscoelastic layered composites. International Journal of Solids and Structures 16 (10), 903–911.

Zhuang, S., 2002. Shock wave propagation in periodically layered composites. Ph.D. Thesis, California Institute of Technology.

Zhuang, S., Ravichandran, G., Grady, D.E., 2003. An experimental investigation of shock wave propagation in periodically layered composites. Journal of the Mechanics and Physics of Solids 51, 245–265.